ICEA

UNIVERSITÀ DEGLI STUDI DI PADOVA

SAFE OPERATIONAL BANDWIDTH OF GAS STORAGE RESERVOIRS
WP2 REPORT

Massimiliano Ferronato
Andrea Franceschini
Giovanni Isotton
Carlo Janna
Pietro Teatini
Omar Tosatto
Claudia Zoccarato

Padova, February 28, 2018

DIPARTIMENTO DI INGEGNERIA CIVILE, EDILE E AMBIENTALE - I C E A
DEPARTMENT OF CIVIL, ENVIRONMENTAL AND ARCHITECTURAL ENGINEERING

Contents

1. Introduction 1

2. Conceptual model 2

2.1 Geometry 2
2.2 Geological/geomechanical setting 3
3. Geomechanical mechanisms to be investigated 4

3.1 Mechanical hysteresis (M1) 4
3.2 Pore pressure distribution in the reservoir (M2) 4
3.3 Fault "lubrification" in non-sealing faults (M3) 5
3.4 Pore pressure variation versus time (M4) 5
4. Parameter variability and model outcomes 6

4.1 Parameter variability 6
4.2 Model Outcomes 7
References 7

1. Introduction

The project “Safe operational bandwidth of gas storage reservoirs” is aimed at investigating the geomechanical hazards and risks associated with gas storage in Underground Gas Storage (UGS) reservoirs. In particular, the aim of the research activities is to investigate how possible drivers of fault reactivation can combine in UGS to increase the hazard of (significant) seismic events and/or even induced "un-expected" (micro-) seismicity.

A summary of WP2 activities is provided in this report. Based on the results of the bibliographic analysis developed in WP1 and the meeting hold in SodM headquarter on February 22nd, 2018, the conceptual model and mechanisms possibly causing fault reactivation have been defined. These simulations will be carried out in WP3.

As defined in the project proposal, the analysis will address the role of: (a) the specific geological settings, such as the geometric configuration and the hydro-geomechanical properties of faults and reservoir; (b) the poroelastic stress changes with respect to the natural stress regime; and (c) the space and time pore pressure gradients in the UGS formation and within the faults bounding/compartmentalizing the reservoir. In particular, the following items have been specified:

- the geometry of the exemplary UGS reservoir and the geological setting;
- the mechanisms that could be responsible for “unexpected” fault reactivations and will be tested by the 3D geomechanical simulator;
- the range of variability of the various geological and geomechanical parameters, together with the pressure evolution due to UGS activities.

This information is described in the following sections.

2. Conceptual model

In this section, the geometry and the geological setting of the UGS conceptual model is presented.

2.1 Geometry

Figure 1 provides a plain view of the selected schematic model. Based on the typical features of the UGS fields in The Netherlands, the reservoir is made of two adjacent square blocks, 2000 × 2000 m wide. The reservoir is confined laterally by four sealing faults, namely F1, F2, F4 and F5. Another fault, F3, potentially subdivides the reservoir in the two compartments, where the pore pressure change Δp_1 and Δp_2 can differ. The reservoir is embedded in a 30 km wide square domain, with its size much larger than the reservoir dimension to minimize the effect of the boundary conditions on the solution in the area of interest.

Faults F4 and F5 are vertical faults, while F1 and F2 are inclined as shown in Figure 2 with a dip angle equal to ±10°. The dip angle of fault F3 can vary within the range [-25° – +25°]. The reservoir is 200 m-thick and 2000-m deep. The bottom of the model is 5000 m deep and the land surface is located at the elevation of 0 m. The faults extend from -3000 m to 1600-m depth, i.e. they terminate within the caprock sealing the reservoir. Notice that block 2 can moved in the vertical direction with an offset of 100 m and 200 m, corresponding to half the thickness and the entire thickness of the reservoir. Along the direction orthogonal to the main F1, F2, and F3 faults (i.e., along the B-B direction of Figure 1), the elevation of the reservoir and caprock formations remain constant.

Standard conditions with zero displacement on the outer and bottom boundaries are prescribed, whereas the land surface is a no-stress boundary.

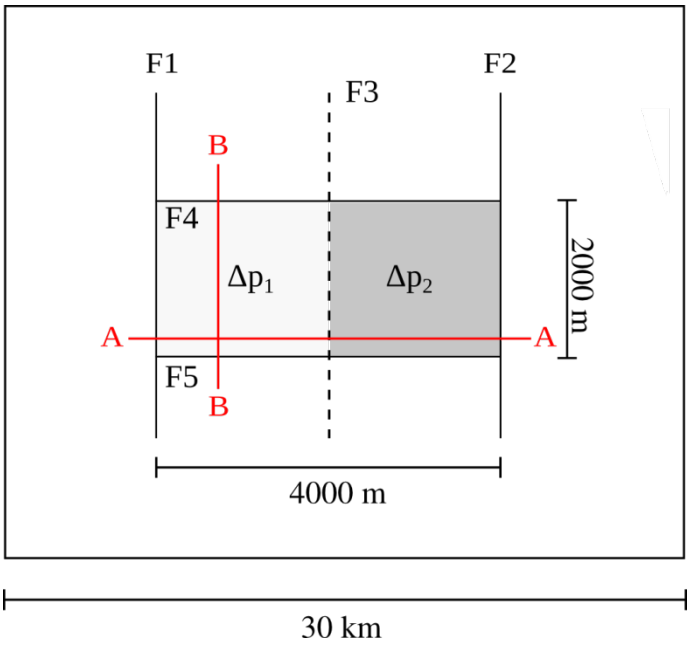

Figure 1 Plan view of the conceptual model.

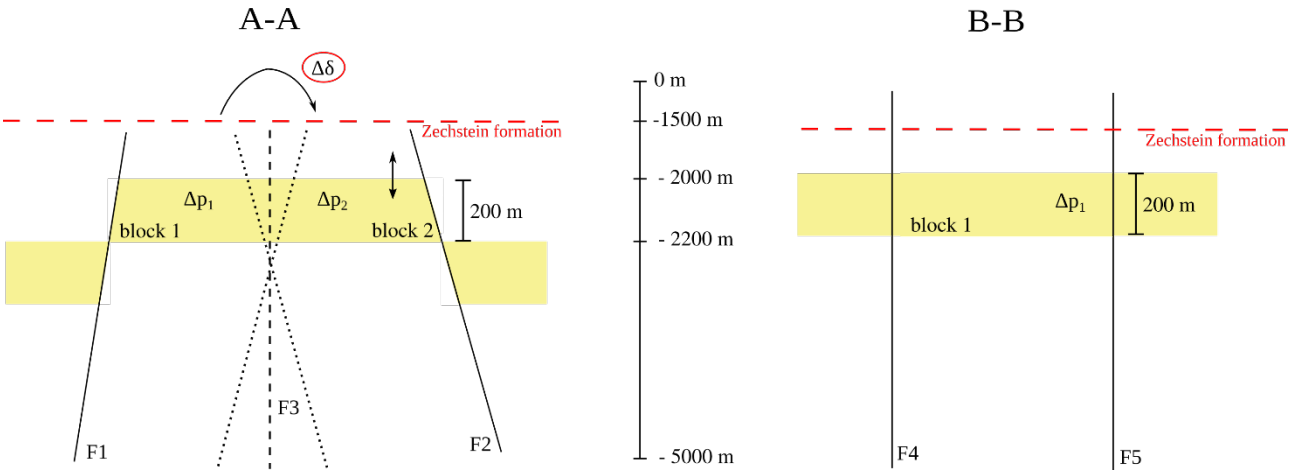

Figure 2 Vertical sections of the conceptual model along the trace A-A and B-B shown in Figure 1.

2.2 Geological/geomechanical setting

The geological and geomechanical setting are characterized as follows:

- initial stress regime: the direction of the principal stresses correspond to the *x*, *y*, and *z* axes of the domain, i.e. θ=0° or θ=90° (Figure 3). According to the dataset provided by SodM, the gradient for the vertical stress is layer-dependent (see Table 2), with the ratios $M_1=\sigma_h/\sigma_v$ and $M_2=\sigma_H/\sigma_v$;
- the failure criterion governing the fault reactivation is characterized by (Figure 3): cohesion (*c*), static (φ_s) and dynamic friction coefficient (φ_d), and critical slip displacement (d_c);
- the reservoir formation, overburden, and underburden are linear elastic media; the caprock can behaves either as a linear elastic or viscous salt (Zechstein formation) layer;
- because of mechanical hysteresis, Young modulus in loading condition (E_I) differs from that in the unloading/re-loading phases (E_{II}).

The value or the variability interval of the various parameters are specified in Section 4.1.

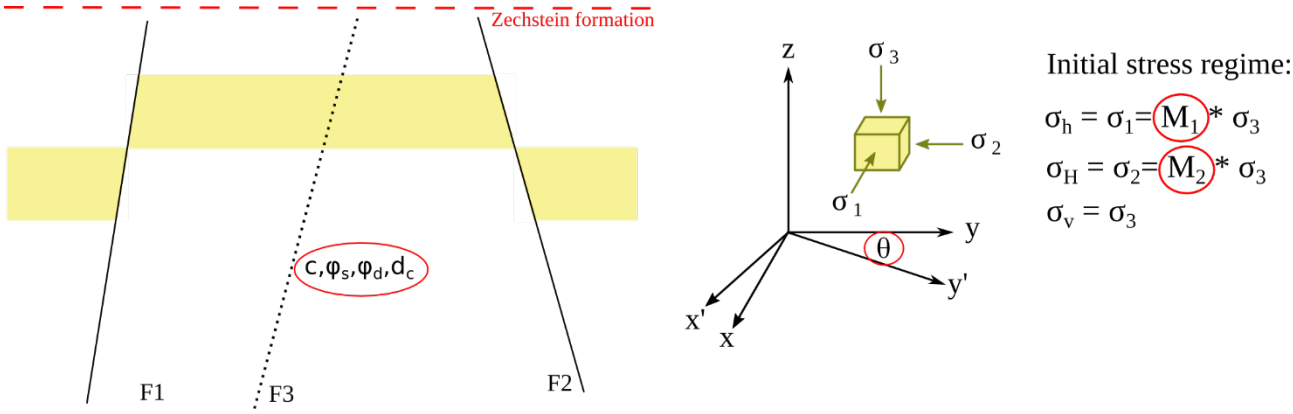

Figure 3 Main parameters use to characterize the fault behaviour and the initial stress regime.

3. Geomechanical mechanisms to be investigated

A number of four mechanisms will be investigated by the geomechanical simulator in the 3D setting described above to the potential root of unexpected seismic events and evaluate the safety (or, in other words, the most critical factors) of UGS in relation to induced seismicity.

3.1 Mechanical hysteresis (M1)

Because of mechanical hysteresis, during unloading-reloading phases the reservoir becomes stiffer than in the loading condition, while the mechanical properties of the surrounding rock remains unaltered. For a same (absolute value of) pressure change, the variation of the stress field within the reservoir can be larger during injection/UGS phase than production because of its larger rigidity in the former condition.

The effect of changing the ratio E_{II} / E_I, with E_{II} / E_I $\geq$ 1, during primary production and unloading/re-loading phases will be tested.

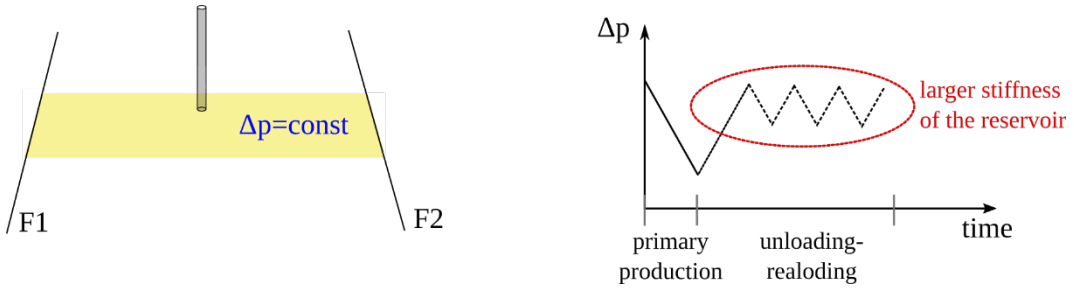

Figure 4 Mechanism 1: stress redistribution because of a stiffer reservoir during cushion gas injection and UGS cycles.

3.2 Pore pressure distribution in the reservoir (M2)

The spatial gradient of the pore pressure change Δp within the reservoir blocks can depend significantly on the injection/production rate. Therefore, the effective stress vs total stress distributions at the faults can differ significantly or not from that within the reservoir compartments, enhancing or not the fault instability.

The effect of changing the injection/production rates during a UGS cycle will be tested.

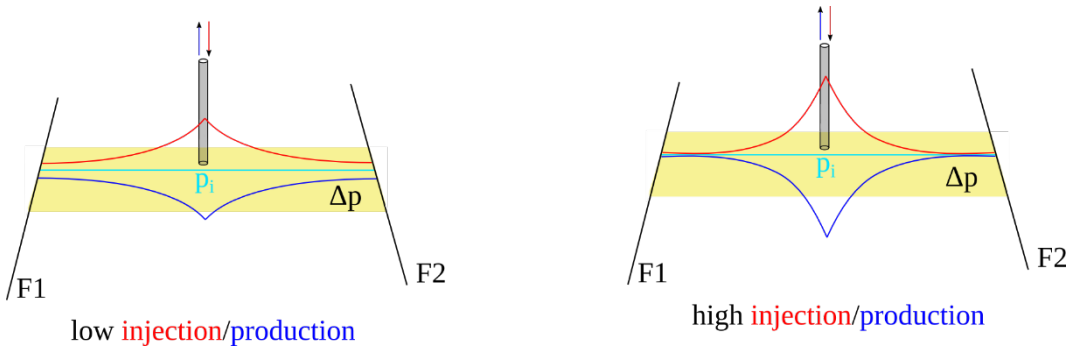

Figure 5 Mechanism 2: the spatial gradient of the pore pressure change can vary significantly within the reservoir depending on low / high injection or production rates.

3.3 Fault "lubrification" in non-sealing faults (M3)

During injection, pore pressure can propagate within non-sealing faults, reducing the effective stress normal to the fault plane and, therefore, favouring their reactivation.

A number of scenarios will be run where the pressure change Δp_3 (Figure 6) in the fault zone, in correspondence of the reservoir depth interval, will be alternatively equal to the maximum, minimum, or average value of the pressure change in the two compartments. A simple 2-D model will be applied to understand the possible Δp_3 upward and downward propagation from the reservoir depth during a UGS cycle. The permeability and stiffness values for the fault material will be derived from the literature (e.g., Zbinden et al., 2017).

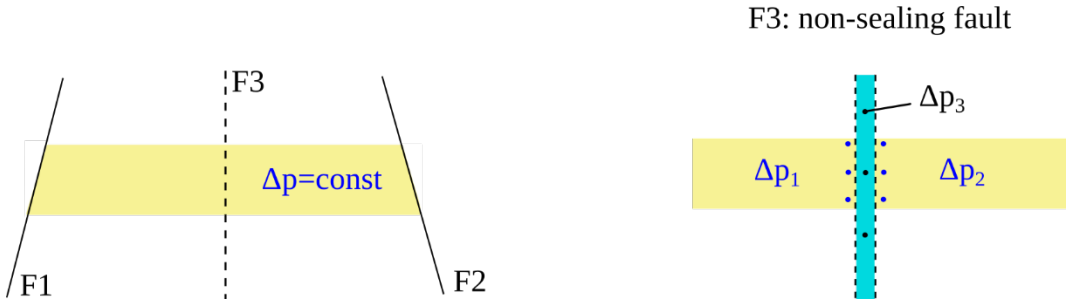

Figure 6 Mechanism 3: the pore pressure change can propagates in a permeable finite-thickness fault zone.

3.4 Pore pressure variation versus time (M4)

A larger pressure change per unit of time, i.e. a faster recovery of the initial pressure during cushion gas injection or a larger pressure fluctuation during UGS cycles, can produce more significant (micro- seismic events because a larger fault area can be "simultaneously" reactivated.

The effect of different Δp during a UGS cycle will be tested.

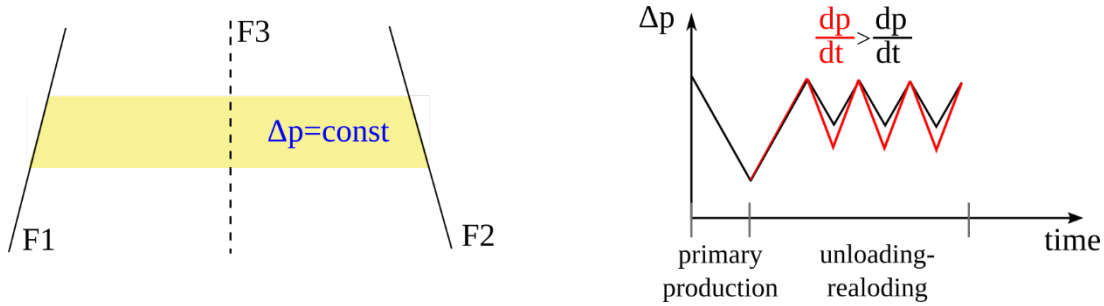

Figure 7 Mechanism 4: a larger pressure change per reference time can activate a larger portion of a fault.

4. Parameter variability and model outcomes

4.1 Parameter variability

With reference to the conceptual model and mechanisms described above, Table 1 summarizes the values of the various parameters that will be investigated in the set of simulations carried out in WP3. The formation-dependent parameters are provided in Table 2.

Table 1 Value and variability range of the various parameters that will be tested in WP3.

PARAMETER	FIXED / VARIABLE	VALUE / INTERVAL
F3 dip	V	0° ; +65°
compartment offset	V	0 ; 100 m ; 200 m
θ	V	0° ; 90°
vertical stress gradient	F	formation dependent (Table 2)
M_1 , M_2	V	0.85 ; 0.90 or 0.65 ; 0.69
c	V	0 ; 10 bar ; 100 bar
φ_s	V	20° ; 30°
φ_d	V	10° ; 17°
d_c	V	2 mm ; 20 mm
E	F	formation dependent (Table 2)
ν	F	formation dependent (Table 2)
E_{II} / E_I	V	1 ; 2.5
caprock	V	linear elastic ; viscous
injection/production rate	V	from SodM (high / low)
Δp_1, Δp_2	V	0 ; 100 bar ; 200 bar
Δp_3	V	Δp_1, Δp_2, $0.5(\Delta p_1 + \Delta p_2)$

Table 2 Formation-dependent geomechanical parameters that will be tested in WP3.

LAYER	DENSITY (kg/m3)	YOUNG MODULUS (GPa)	POISSON RATIO
Overburden	2200	10.0	0.25
Zechstein Salt	2100	40.0	0.3
Reservoir (Upper Rotliegend)	2400	15.0 ; 25 ; 40	0.2
Underburden	2600	30	0.2

Concerning the Zechstein formation, the isotropic stresses will be addressed by using $M_1=M_2=1$, with a Maxwell viscosity in the range 10^{-16} – 10^{-17} Pa·s.

4.2 Model Outcomes

Because of the possible combinations of the parameters listed in Table 1and Table 2, WP3 will deliver a large amount of modelling results. The main output that will be used to check the safety of the gas storage will be the following:

- activated faults:
  - A (area of the activated part),
  - δ_{max} (maximum sliding),
  - δ_{avg} (average sliding of the activated area),
  - $M_0= G \times A \times \delta_{avg}$ (seismic moment), with G the shear modulus of the rock hosting the fault;
- inactive faults:
  - χ_{min} (minimum value of the safety factor χ),
  - χ_{avg} (average value of the safety factor χ);

  where $\chi=1 - \tau / \tau^*$, with τ the actual tangential stress on a fault element and τ^* the limit tangential stress according with the Mohr-Coulomb criterion.

References

Zbinden, D., A. P. Rinaldi, L. Urpi, and S. Wiemer (2017), On the physics-based processes behind production-induced seismicity in natural gas fields, J. Geophys. Res. Solid Earth, 122, 3792–3812.